Microelectronics Reliability 119 (2021) 114067

Contents lists available at ScienceDirect

Microelectronics Reliability

journal homepage: www.elsevier.com/locate/microrel

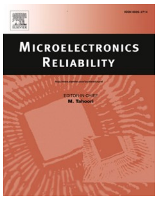

Rolling reliability of polyurethane and polyurethane-acrylic ICAs interconnections on printed stretchable electronics

Zhao Fu, Vänni Panula, Behnam Khorramdel, Matti Mäntysalo [*]

Faculty of Information Technology and Communication Sciences, Tampere University, 33720 Tampere, Finland

A R T I C L E I N F O

Keywords:
ICA
Rolling test
Reliability
Failure mechanism
Stretchable electronics
Printed electronics

A B S T R A C T

In this study, bending reliability of the surface mounted devices (SMD) attached using isotropic conductive adhesive (ICAs) on screen printed stretchable devices polyurethane substrate are investigated. The performance of polyurethane and polyurethane-acrylic ICAs and the impact of rolling speed are studied. The rolling test was performed using the customized automatic rolling test device. It was found that the polyurethane-acrylic blend gives poorer adhesion with the silver conductor and very high cohesive force. The polyurethane resin brings adhesive high adhesive force with the silver conductive layer while lower adhesion with the Tin surface of the SMD, and it exhibited poorer cohesive force. The resistance of all samples experienced a steady and slow increase period before it accelerated to failure. During the slow and steady increase phase, the increased resistance was mainly from the conductive layer, whereas during the dramatic increase phase, it was mainly from the ICA connected area. The increased rolling speed had accelerated the resistance evolution process and lowered the samples' reliability severely. It also lowered the adhesion of the polyurethane-acrylic blend with the ink layer and lowered cohesive force of polyurethane ICA.

1. Introduction

With the increasing demand for applying electronics to the areas with complex shapes, the stretchability of the electronics has been increasingly concerned. Improving the stretchability of the electronics from materials, structure, connection, and fabrication has been a focus of research [1]. As an example, stretchability can enable electronics to be applied to the human skin and textiles [2]. The human skin normally moves with strain of 15–20% [3], which would require the electronic device to be able to endure mechanical deformation and can recovery. Printed Electronics (PE) has been used to fulfill this demand with advantages in packaging stacks of micro components or devices on the substrate, providing flexibility and ductility, reduced use of resources, lower fabrication temperature and lower cost [4,5]. The common printing methods include screen printing [6], inkjet printing [7], flexography printing [8], and gravure printing [9]. Screen printing is a process in which the ink is pressed through a stenciled mesh screen with designed pattern to create a printed pattern. It has been reported to be advantageous for fabricating the conductive ink for stretchable electronics [10,11].

The stretchable nature also demands good reliability. For the conventional electronics and flexible electronics, intensive study of failure mechanisms have focused on the interconnects [12–15], which have also found be easy to fail in the electronic device [16–18]. For stretchable electronics, some design of interconnects have been investigated, such as embedding metal wire in stretchable substrate material [19] and ultra-stretchable Arcimedean interconnects [20]. ICA has been reported [21,22] to be promising alternative to the traditional soldering for interconnecting the electronic components due to its environmentally friendly nature and low processing temperature. Therefore, in this study, we focus on the reliability and failure behavior at ICA connected area in stretchable electronics.

So far, the reliability study of stretchable electronics has been mainly focused on the environmental tests and stretching test. Researchers have studied the mechanical reliability of flexible electronics by customizing the tests and devices. Klein et al. [23] created prototype using bladder expansion for testing mechanical reliability. Moser et al. [24] customized an open-source tensile tester with toy bricks for stretchable electronics. Chen et al. [25] studied the reliability of stretchable interconnect by simulating bending and stretching. Bossuyt et al. [26] investigated the reliability of stretchable circuit board with cyclic stretching test with 20% strain and observed the fatigue-like failure.

---

* Corresponding author.
E-mail address: matti.mantysalo@tuni.fi (M. Mäntysalo).

https://doi.org/10.1016/j.microrel.2021.114067
Received 11 October 2020; Received in revised form 29 January 2021; Accepted 11 February 2021
Available online 2 March 2021

Park et al. [27] developed highly stretchable Ag conductor which was printed on PU substrate, and it survived the cyclic stretching test of 10,000 cycles at 40% strain with 3 mm bending radius. However, such mechanical tests for stretchable electronics remains lacked.

In addition to the conventional reliability tests mentioned above, the behavior of the samples during the rolling should also be investigated. Because rolling is inevitable for stretchable electronics devices integrated to textile. In this study, we present a customized automatic rolling test device which is used to do all the cyclic rolling tests. The aim is to figure out the impacts of the ICA's binder and rolling speed on the reliability and failure mechanisms of the ICA in the screen printed stretchable electronics.

2. Research materials & methods

2.1. Sample components

The sample consists of a 100-μm thick, highly stretchable thermoplastic polyurethane (TPU) substrate (Platilon U4201, Epurex Films), screen printable highly conductive & stretchable silver ink (CI-1036, Engineered Conductive Materials), ICAs (DZP SA0850 from DZP Technologies, Dycotec DM-SAS-10010 from Dycotec Materials), and SMD (zero ohm chip resistor SR2512E4A-ZERO-TIN with dimension 8.10 mm × 3.50 mm × 0.55 mm). The DZP SA0850 has polyurethane-acrylic blend with 10,000–15,000 mPa.s viscosity, while the Dycotec DM-SAS-10010 has polyurethane resin with 3–7 mPa.s viscosity, which is their main difference.

2.2. Sample fabrication

The samples were fabricated using Ekra X5 Professional automatic screen printer, the procedure is illustrated in Fig. 1. The TPU with flexible sheet carrier was placed flatly on the printing table with vacuum on (step 1), which was then moved into the printing area under the mesh screen. The substrate shall be aligned with the screen pattern. The squeegee was then adjusted to just touch the mesh screen slightly with 200 N squeegee pressure, and to print the conductive ink by moving forwards and backwards over the screen pattern for 2 cycles with a speed of 100 mm/s with 2 mm snap off distance (step 2). The printing was performed in 21 °C temperature and 55% relative humidity environment. The printed conductive layer was cured in the oven at 130 °C for 30 min (step 4). After air cooling to the room temperature, the TPU substrate was removed from the carrier sheet before it was cut into the final sample size (steps 5 and 6). Next, the TPU substrate was taped on a aluminum plate for ICA and SMD assembly. The ICA was applied sufficient to cover two rows of the conductor pad width by using manual dispenser (step 7). The SMD was assembled manually using the tweezers. Afterwards, the samples were cured in the oven (with DZP SA0850, the sample was cured at 120 °C for 30 min and with Dycotec DM-SAS-10010, the sample was cured at 120 °C for 60 min) as recommended by the manufacturers. By then, the sample is fabricated, as shown in Fig. 2(A). The sample pattern was designed as presented in Fig. 2(B). The ink layer was designed to be 2 mm wide. The electrical resistance of the fabricated samples was verified using Keithley 2425 multimeter.

2.3. Experimental plan

The cyclic rolling test was planned and conducted as described in Table 1. All the samples share the same substrate, conductive ink, and SMD, as introduced in section A. The reference samples share the same pattern and dimensions as other samples except the SMD connected is short circuited with conductive ink printed but without any open circuit for component assembly.

2.4. Automatic rolling test with customized equipment

The cyclic rolling test was conducted by the customized automatic rolling test device, as presented in Fig. 3. The system was designed and

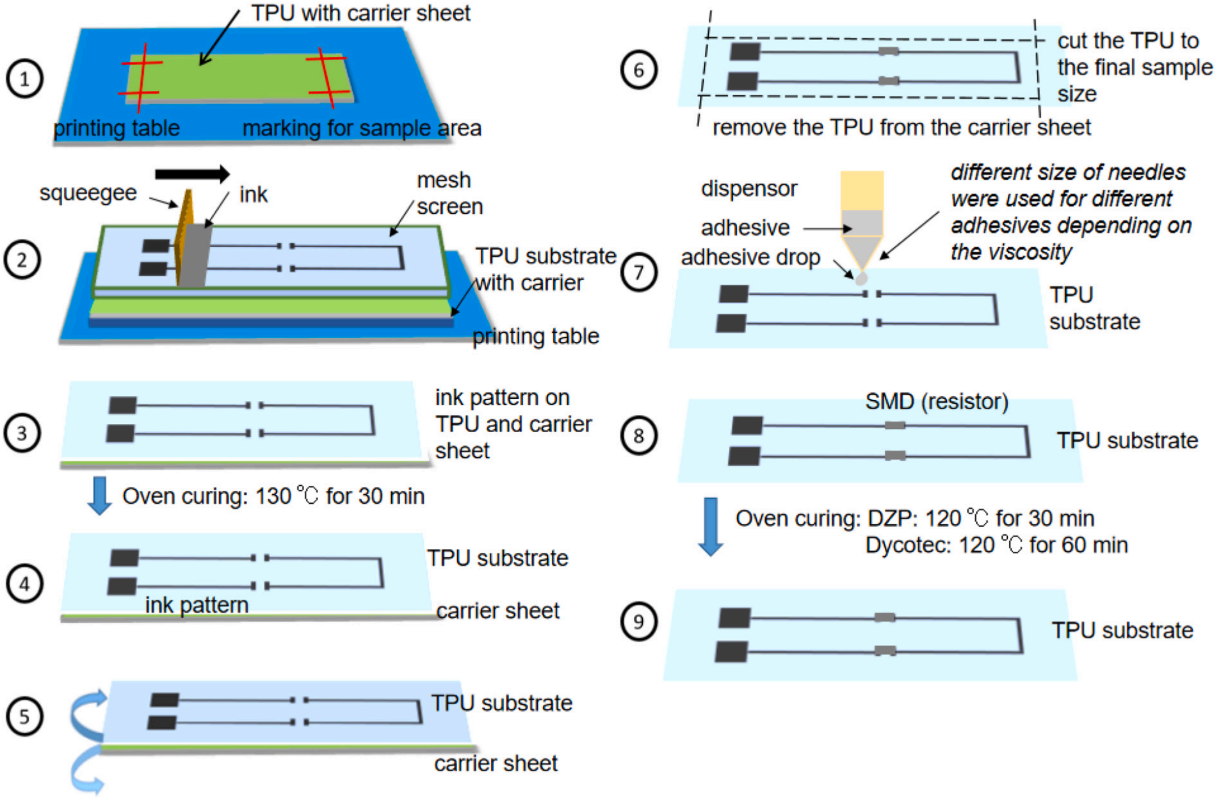

Fig. 1. Schematic diagram of the fabrication procedure of screen printed stretchable electronics samples for rolling test.

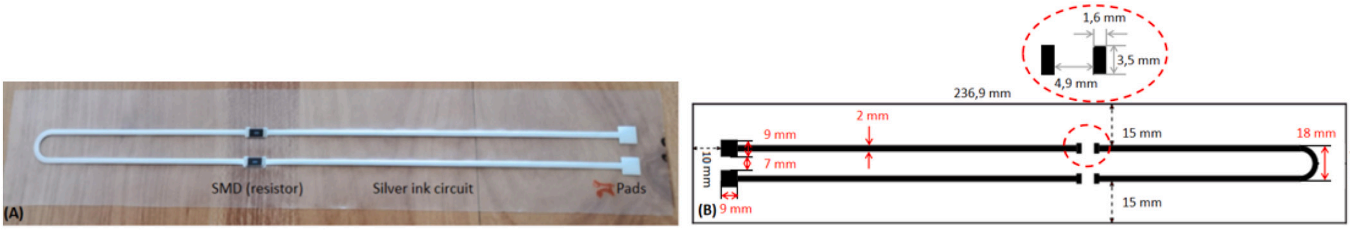

Fig. 2. (A) A screen printed stretchable electronics sample and (B) the dimensions of the samples and pattern.

Table 1
Rolling test plan for printed stretchable electronics.

ICAs	Mandrel radius	Rolling speed	Quantity of samples
DZP (polyurethane-acrylic blend)	20 mm	20 mm/s	10 pcs
	20 mm	50 mm/s	10 pcs
Dycotec (polyurethane)	20 mm	20 mm/s	10 pcs
	20 mm	50 mm/s	10 pcs
No adhesive (reference samples)	20 mm	20 mm/s	3 pcs
	20 mm	50 mm/s	3 pcs

manufactured at Tampere University under the guidance of standards IPC-9204 [28] and ASTM F3147-15 [29]. The control board is powered by supply voltage +11 V, and it is connected to the two pads of the sample through the copper board on the clamp with a conductive tape in between. The clamp used for fixing the sample is designed with a hollow middle part so that the rubber parts of the clamp can stabilize the two sides of the TPU substrate while the conductive circuit can go through the hollow part without being extruded nor broken. The sample moves upwards and downwards repeatedly, powered by two stepper motors. The rolling movement ensures SMD to go over the mandrel. Meanwhile, the real-time resistance is monitored by the control board. A pull-up resistor with 4.68 kΩ resistance is used, which determine the upper threshold value of the resistance to be around 520 Ω. The test stops when the resistance reaches the upper threshold or when the resistor is suddenly delaminated from the ICA. Then, the four ICA connected areas were imaged by the ordinary camera when the sample was over the mandrel for analyzing the failures.

In this process, the resistance was measured as illustrated in Fig. 4. The parameters of rolling speed and resistance value of the configuration resistor were set in the software, and sent to the control board, which is made of Arduino Mega R3 due to its availability and relatively high performance. The control board powers the two stepper motors, which drive the sample rolling through leather belts. The voltage goes through the sample, amplified by preamplifier, and then goes to the control board. The sample's real resistance is calculated and then stored to the memory card.

3. Results and discussion

3.1. Evolution of resistance during rolling test

The resistance data was pre-processed with moving average filter of 5 neighboring data in order to reduce random noise. The average values were used for plotting the graph with the corresponding cycle of test. Three reference samples consisting of only conductive ink circuit without any resistor, were tested at 20 mm/s, three were tested at 50 mm/s. The Resistance - Number of Cycles graphs of the three samples tested at the same rolling speed were highly similar, and one representative graph was selected as demonstrated in Fig. 5. It shows that with 20 mm/s rolling speed, the resistance increased slowly from around 7 Ω

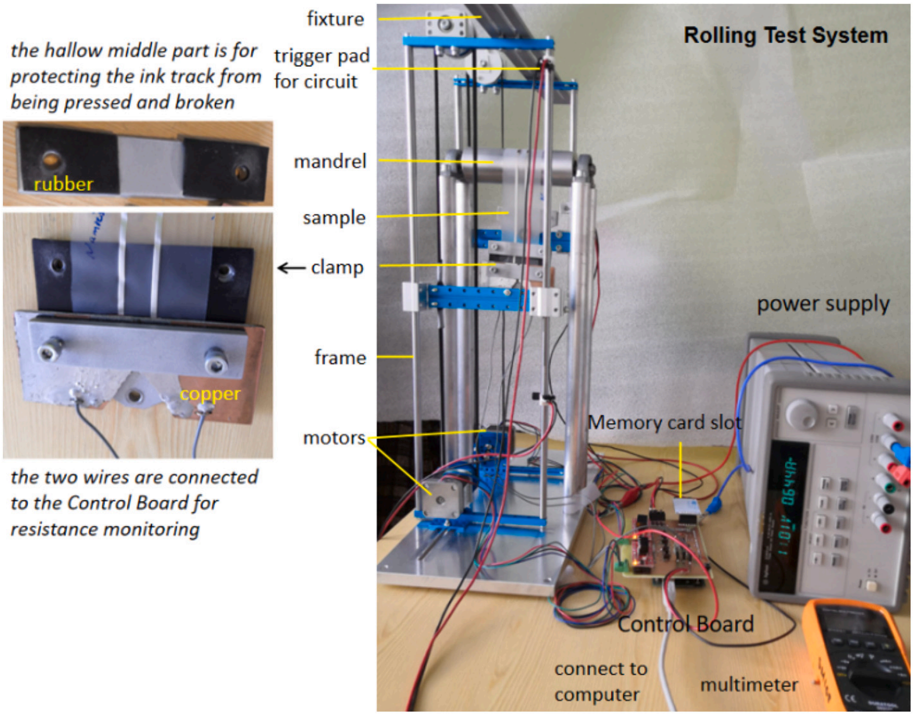

Fig. 3. The customized automatic rolling test system and the hollow design of the middle area of the clamp.

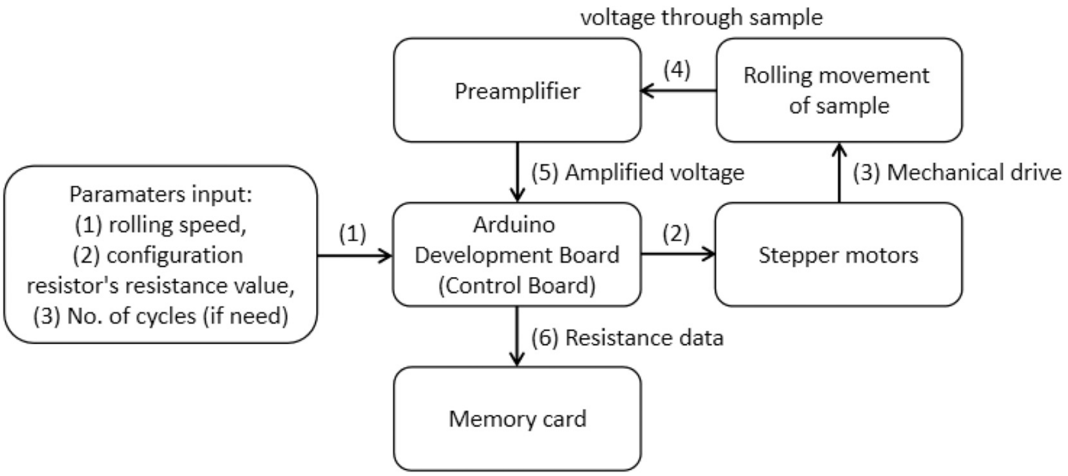

Fig. 4. Flowchart showing the mechanism of resistance measurement during rolling test.

to 20–25 Ω within 20,000 cycles of test, while with 50 mm/s, the resistance increase is obviously at higher level and experienced a dramatic increase of resistance after the slow increase phase of around 8000 cycles of test. The figure also indicate that the resistance of the conductive track did increase with the increase of the test cycle.

Fig. 6 shows typical sample's graph of each case. For the 10 samples with DZP adhesive tested at 20 mm/s, six samples showed a steady and slow resistance increase for 1000–6000 cycles, and then accelerated to failure in 2400–8000 cycles. However, the other four samples showed a steady and slow resistance increase up to 8000–26,000 cycles, and then accelerated to failure in coming 3000 cycles. For the ten DZP samples tested at 50 mm/s, five samples experienced a steady and slow resistance increase for 4000–5000 cycles before accelerated to failure in a small number of cycles. The other five samples experienced a little shorter period of resistance increase and then accelerated to failure in a larger number (2600–5600) of cycles. It indicates that, with higher rolling speed, the reliability was significantly lower, and the resistance acceleration phase takes up a significantly higher portion of the whole test phase.

Ten samples with Dycotec adhesive were tested at 20 mm/s, and ten were tested at 50 mm/s. One of each case failed due to the data corruption, which was left out in analysis. For the test at 20 mm/s, six out of nine samples experienced a large number of cycles (mostly within 15,000–27,000) of steady and very slow increase of resistance, and then accelerated to the failure in a relatively smaller number of test cycles (1000−10,000); two out of nine samples failed to sudden and completed delamination of SMD from the adhesive; and one out of nine sample survived an exceptionally large number (42610) of rolling test. For the test at 50 mm/s, five out of nine samples' resistance increased steadily and slowly for 4000–7000 cycles, and then accelerated to failure in 3000–6000 cycles of test; three out of nine samples failed to sudden and completed delamination of resistor from the adhesive. The resistance of the one out of nine sample experienced a slow increase until 10,500 cycles of test and then accelerated to failure in 3000 cycles. This also reveals that the higher speed of rolling had shortened the lifespan and lowered the reliability and increased the portion of the resistance acceleration phase against the whole test phase.

By comparing the different behaviors of the different samples in four cases, it is clear that all samples experienced a steady and slow increase of resistance, and then went through a dramatic increase of resistance until failure. Besides, with higher rolling speed, the resistance increase is greater for both DZP and Dycotec cases. In addition, for both DZP and Dycotec samples with lower rolling speed, they survived significantly more cycles of test before the acceleration of the resistance, while they tend to be accelerated to failure within a relatively smaller number of cycles of test; but with higher rolling speed, the resistance acceleration.

phase takes a larger portion of the whole test phase. Because during the cyclic rolling or bending test of electronics, the resistance can increase at some point due to the crack expansion within the conductive track layer while the resistance recovered to almost the same low level when it is released. This phenomenon has been widely reported by A. Korhonen [30], T. Happonen [31], J. Suikkola [11], and F. Bossuyt [26].

To gain a better understanding of the resistance evolution behavior of different types of samples, the Resistance-Number of Cycles graphs of typical samples of each test case are compared in Fig. 7. It shows that the reference samples and ICA assembled samples exhibit highly similar resistance evolution when tested at the same rolling speed, whereas the increased rolling speed has accelerated the increase of resistance significantly. These indicate that the steady and slow increase of resistance is mainly attributed to the conductive ink track rather than the ICA

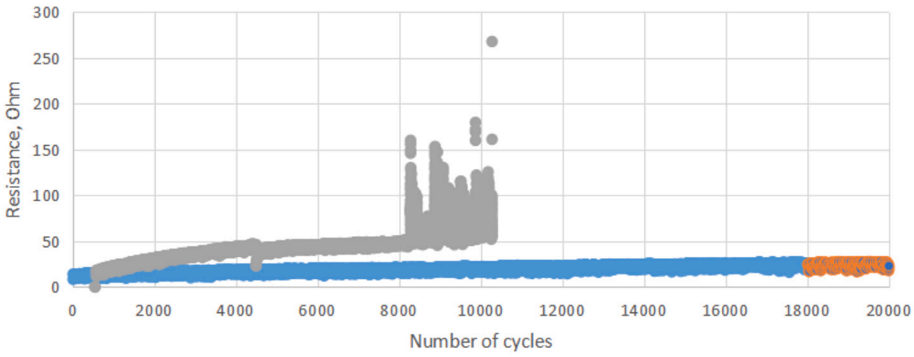

Fig. 5. Representative Resistance - Number of Cycles graphs of rolling test of reference samples at different rolling speeds.

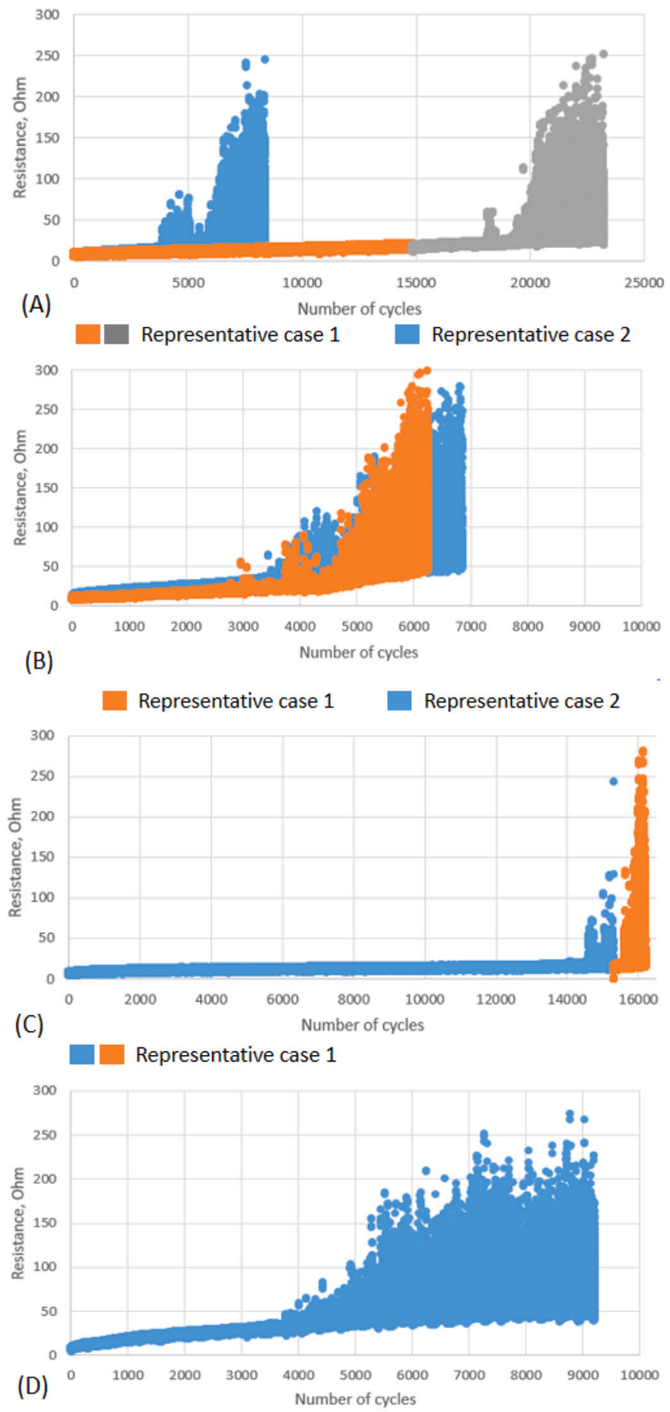

Fig. 6. Representative Resistance - Number of Cycles graphs of rolling test of (A) DZP sample tested at 20 mm/s, (B) DZP sample tested at 50 mm/s, (C) Dycotec sample tested at 20 mm/s, (D) Dycotec sample tested at 50 mm/s. *(NB: in fig. A, there are two representative graphs, the orange and gray make one graph due to the limitation of large amount of data from one test, blue graph is another case. In fig. B, there are two graphs, representing two kinds of cases. In fig. C, the two colors make one graph due to the same reason.)*

attached area.

3.2. Reliability

In each test, the data of the average resistance value and the number of cycles were plotted. The resistance of all tested samples grew slowly for a relatively long phase before it accelerated dramatically to the failure, as shown in Fig. 6. To study the reliability in different test cases, the numbers of the test cycle when the sample failed are summarized in Fig. 8. The figure shows that when tested at 50 mm/s, the samples survived remarkably smaller number of rolling cycles. In addition, when the reliability of the samples with two ICAs are compared, the samples with Dycotec adhesive generally exhibit higher reliability than that with DZP adhesive before the resistance acceleration and before the failure regardless of rolling speed.

3.3. Failure mechanisms

The images of the failed areas in the tested samples were taken by ordinary camera after the test stopped and while the sample was still on the mandrel. Ten tests of each type of test case were successful, except the test of one sample with Dycotec adhesive when tested at 20 mm/s failed (this case was not taken into account). The failure cases are summarized in the pie charts of Fig. 9, some representative failures are presented in Fig. 10.

It was found that the samples with DZP adhesive only failed by delamination of SMD-ICA interface and ICA-ink layer interface, while with Dycotec adhesive, except the above two interface delamination, the failure mechanisms also include the ICA crack (mostly horizontal crack in the middle). With DZP adhesive, the dominant failure mechanism is ICA-ink layer interface delamination, especially when tested with 50 mm/s which contains 73% of all failure cases. With Dycotec adhesive, the samples mainly failed by SMD-ICA interface delamination, which takes over 60% of all failures. The distinct difference in the dominant failure mechanisms of the samples with two adhesives reveal that polyurethane had enabled Dycotec adhesive to achieve a stronger adhesion with the silver layer while a weaker adhesion with the metal Tin on the surface of the resistor compared with DZP adhesive. The cracking of the Dycotec adhesive also reveal that the polyurethane resin exhibits lower cohesion than the polyurethane-acrylic blend.

The rolling speed had obvious impact on the failure mechanisms. The increased rolling speed increased the ICA-ink layer interface delamination from 57% to 73% while decreased the SMD-ICA interface delamination from 43% to 27% of DZP samples. It is because with higher rolling speed, the stretched ICA-ink interface had less time for recovery. The SMD-ICA interface delaminaion reduced due to the earlier delamination at the ICA-ink interface. This reveals that the polyurethane-acrylic blend achieved a weaker adhesion with silver layer than with Tin. Because the relatively higher viscosity of the DZP SA0850 adhesive led to a larger contact angle with the silver conductive layer and lower surface energy and weaker adhesion with the silver layer. The absence of the adhesive cracking failure exhibits its high cohesive force. These two features together is a lyophobic condition [32]. The increased rolling speed increased the Dycotec adhesive horizontal cracking from 11% to 26% while reduced the ICA-ink layer interface delamination from 26% to 3%. However, the increased rolling speed did not significantly influence the dominant failure mechanism of SMD-ICA interface delamination. This shows that the faster rolling weakened the cohesive force within the Dycotec adhesive, which is rooted in the intermolecular forces among the polyurethane binder. The low viscosity (3–7 mPas) of the Dycotec DM-SAS-10010 adhesive achieved very smaller contact angle with the silver layer and high surface energy at the adhesive-ink layer interface, which creates high surface tension and micro-mechanical adhesion. This explains the small portion of ICA-ink layer interface delamination. The cohesive force is achieved through chemical bond, crosslinking of the polymer's intermolecular interactions and interactions among the molecules. The polyurethane-acrylic blend reached higher molecular interaction compared with the pure polyurethane resin. This explains why Dycotec adhesive was subjected to cohesive failure while DZP adhesive did not. The strength and the stretchability of the DZP SA0850 and Dycotec DM-SAS-10010 have not been known, the further research in these is recommended. It has been reported that the cohesive strength of the adhesive, rather than the

]

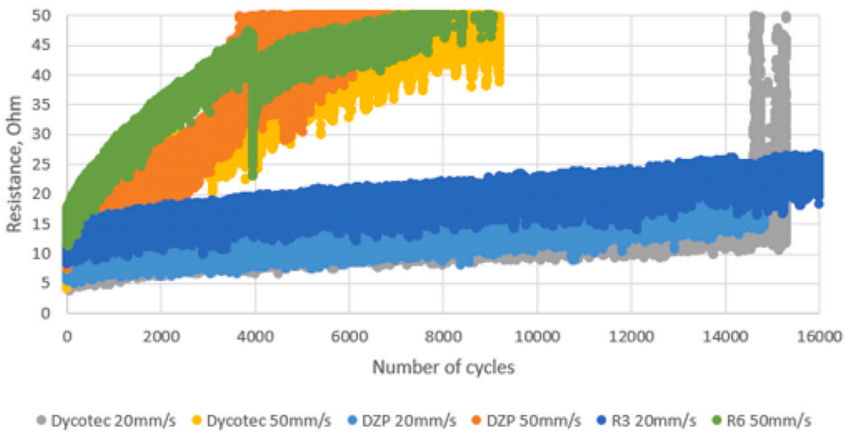

Fig. 7. Resistance evolution of the representative samples of different test cases during cyclic rolling.

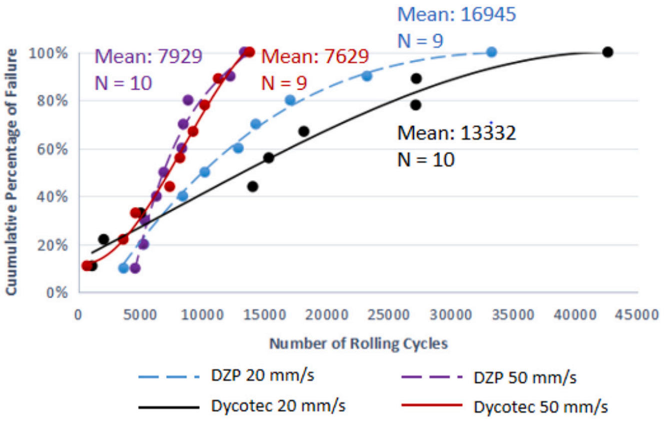

Fig. 8. Empirical cumulative distribution function of number of cycles when failure occurred to DZP and Dycotec samples.

adhesion between the adhesive and substrate, can limit the bonding strength [32].

4. Conclusion & future work

In this research, the impact of the ICA's resin and the rolling speed on the reliability and failure mechanism of the printed stretchable electronics was investigated using the customized automatic rolling test device. The two ICAs based on polyurethane-acrylic blend (DZP SA0850) and polyurethane (Dycotec DM-SAS-10010) were used. The conductive layer was fabricated by screen printing and the ICAs were applied using manual dispenser. The failure images were taken by ordinary camera after the test stopped and while the sample was over the mandrel.

The increased rolling speed was found to lower the sample's reliability severely by acceleration of resistance increase. The increased rolling speed influenced the failure mechanisms of different ICAs differently due to different adhesion and cohesion of polyurethane and polyurethane-acrylic blend of the ICAs. Compared with polyurethane, the polyurethane-acrylic blend exhibits poorer adhesion with the silver conductive layer than the polyurethane, but it exhibits better cohesion. The samples were mainly subjected to the cohesive failure of the ICA and adhesive failure at the ICA-SMD interface and ICA-ink layer interface. The failure mechanisms are also clearly impacted by the ICA's resin.

During the cyclic rolling, the samples of all cases experienced a relatively long period of slow and steady increase of resistance before they accelerated to failure. During the slow and steady increase phase, the resistance increment is mainly from the conductive ink track rather than the SMD and ICA. During the dramatic increase phase, the increased resistance is more due to the SMD and ICA area.

Overall, the Dycotec adhesive exhibits slightly higher reliability. However, due to the different cohesive and adhesive force as summarized above, the selection of the adhesive would depend on the application. In addition, improving the reliability of the conductive ink track (for example in printing and curing) and controlling the rolling speed in the application are recommended. For further understanding, the impact of the mandrel radius and different method for applying ICA on the reliability and failure mechanism can be investigated.

Author contributions

Z.F. conceptualized, designed, and performed this research and experiment, designed the mechanical part of the rolling device, fabricated the sample except screen printing, analyzed the results and wrote

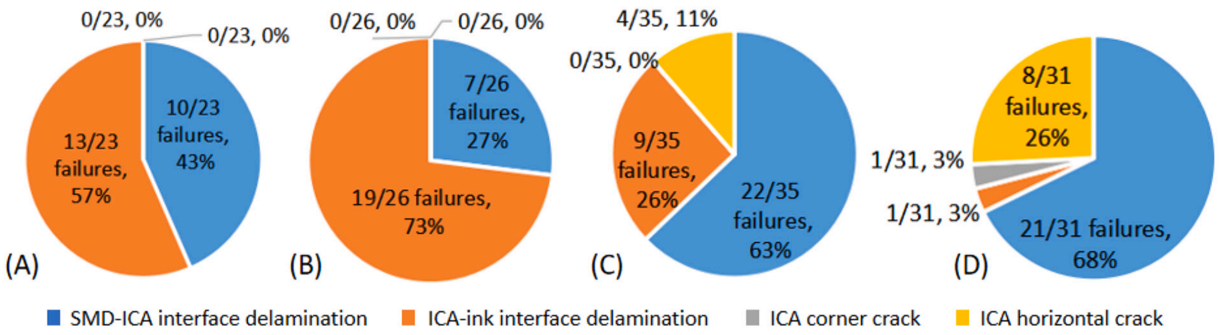

Fig. 9. Failure mechanisms of (A) DZP samples tested at 20 mm/s; (B) DZP samples tested at 50 mm/s; (C) Dycotec samples tested at 20 mm/s; (D) Dycotec samples tested at 50 mm/s during the cyclic rolling tes.

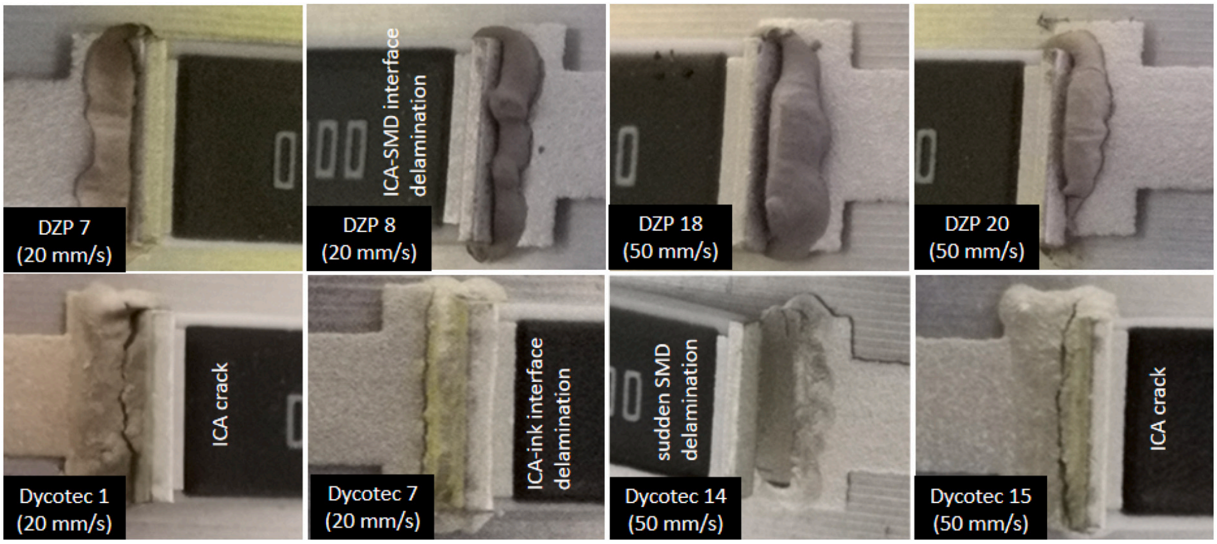

Fig. 10. Representative failures of printed stretchable electronic samples with DZP and Dycotec adhesives after rolling test at different rolling speeds.

the manuscript and finalized the paper. V.P. designed and fabricated the control board and electrical system of the rolling device, B.KH. designed the clamp for the rolling device, provided general guidance to the research and revised the manuscript. M.M. supervised the research and revised the manuscript.

Declaration of competing interest

The authors declare no conflict of interest.

Acknowledgement

This work is funded by Business Finland (Grant Number 2947/31/2018). Parts of the research use Academy of Finland Research Infrastructure "Printed Intelligence Infrastructure" (PII-FIRI, Grant Number 320019). The authors acknowledge Lasse Söderlund for manufacturing the frame part of the rolling test device, and Aleksis Leinonen for screen printing the conductive ink in sample fabrication.

References

[1] M.L. Hammock, et al., 25th Anniversary Article: The Evolution of Electronic Skin (e-skin): a brief history, design considerations, and recent progress, Adv. Sci. 25 (42) (2013) 5997–6038, https://doi.org/10.1002/adma.201302240.
[2] D.-H. Kim, et al., Epidermal electronics, Science 333 (6044) (2011) 838–843 (doi: 10.1126).
[3] B. Huyghe, et al., Design and manufacturing of stretchable high-frequency interconnects, IEEE Trans. on Adv. Packag. 31 (4) (2008) 802–808, https://doi.org/10.1109/TADVP.2008.927811.
[4] J.A. Rogers, A diverse printed Future, Nature 468 (2010) 177–178, https://doi.org/10.1038/468177a.
[5] C. Reese, et al., Organic thin film transistor, Mater. Today 7 (9) (2004) 20–27, https://doi.org/10.1016/S1369-7021(04)00398-0.
[6] A. Larmagnac, *et al.*, Stretchable electronics based on Ag-PDMS composites, Scientific Reports 4, 7254. doi:https://doi.org/10.1038/srep07254.
[7] T. Liimatta, *et al.*, "Inkjet printing in manufacturing of stretchable interconnects" in Proc. 64th IEEE Electro. Comp. Technol. Conf. (ECTC): 151–156. doi:https://doi.org/10.1109/ECTC.2014.6897281.
[8] B.M. Rodriguez. (2016). *Inkjet and Screen Printing for Electronic Applications.* (dissertation) University of Barcelona, Barcelona, Italy.
[9] E. Hrehorova, Materials and Processes for Printed Electronics: Evaluation of Gravure Printing in Electronics Manufacture (Dissertation), Western Michigan University, Kalamazoo, USA, 2007.
[10] A. Mohammed, et al., A stretchable and screen-printable conductive ink for stretchable electronics, Appl. Phys. Lett. 109 (18) (2016) 184101, https://doi.org/10.1063/1.4965706.
[11] J. Suikkola, et al., Screen-printing fabrication and characterization of stretchable electronics, Scientific Report 6 (2016) 25784, https://doi.org/10.1038/srep25784.
[12] S.K.W. Seah, et al., Failure mechanisms of interconnections in drop impact, Electronic Components and Technology Conference (2006), https://doi.org/10.1109/ECTC.2006.1645852, 30.5–2.6. (San Diego, CA, USA).
[13] Q. Lin, et al., Study of interconnect failure mechanism and micro-effort for ULSI, Int. J. Comp. Commun. Eng. 8 (3) (2019) 104–118, https://doi.org/10.17706/ijcce.2019.8.3.104–118.
[14] Y.C. Chan, et al., Failure mechanisms of solder interconnects under current stressing in advanced electronic packages, Progress in Materials Science 55 (5) (2010) 428–475, https://doi.org/10.1016/j.pmatsci.2010.01.001.
[15] N. Palavesam, et al., Influence of flexibility of the interconnects on the dynamic bending reliability of flexible hybrid electronics, Electronics 9 (2) (2020) 238, https://doi.org/10.3390/electronics9020238.
[16] R.R. Keller, et al., Interconnect failure due to cyclic loading, AIP Conference Proceedings 612 (2002) 119, https://doi.org/10.1063/1.1469897.
[17] S. Shetty, et al., Fatigue of chip scale package interconnects due to cyclic bending, J. Electron. Packag. 123 (3) (2001) 302–308, https://doi.org/10.1115/1.1362673.
[18] A. Skipor, et al., "Mechanical Bending Fatigue Reliability and its Application to Area Array Packaging" *ECTC 51th Conference Proceedings, Orlando, USA*, 2001, pp. 606–612, https://doi.org/10.1557/PROC-682-N5.6.
[19] M. Gonzalez, et al., Design of Metal Interconnects for stretchable electronic circuits, Microelectron. Reliab. 48 (6) (2008) 825–832, https://doi.org/10.1016/j.microrel.2008.03.025.
[20] N. Alcheikh, et al., Ultra-stretchable Archimedean interconnects for stretchable electronics, Extreme Mechanics Letters 24 (2018) 6–13. https://doi.org/10.1016/j.eml.2018.08.005.
[21] A.S.G. Andrae, *et. al.*, "Conductive Adhesive vs. Solder Paste: A Comparative Life Cycle Based Screening", *14th CIRP Conference on Life Cycle Engineering.* 11–13.6.2007, Tokyo, Japan. doi:https://doi.org/10.1007//978-1-84628-935-4_50.
[22] M.J. Yim, et al., Review of recent advances in electrically conductive adhesive materials and technologies in electronic packaging, J. Adhes. Sci. Technol. 22 (14) (2008) 1593–1630, https://doi.org/10.1163/156856108X320519.
[23] S.A. Klein, et al., Mechanical testing for stretchable electronics, J. Electron. Packag. 139 (2017), 020905, https://doi.org/10.1115/1.4036389.
[24] R. Moser, et al., From playroom to lab: tough stretchable electronics analyzed with a tabletop tensile tester made from toy-bricks, Adv. Sci. 3 (2016) 1500396, https://doi.org/10.1002/advs.201500396.
[25] Q. Chen, et al., Reliability study of stretchable electronics interconnect by simulation, in: 11th Intl. Conf. on Electron. Packag. Technol. & High Density Packag. 16-19 August 2010, Xi'an, China, 2010, https://doi.org/10.1109/ICEPT.2010.5582755.
[26] F. Bossuyt, et al., Cyclic endurance reliability of stretchable electronic substrates, Microelectron. Reliab. 51 (2011) 628–635, https://doi.org/10.1016/j.microrel.2010.09.032.
[27] J.Y. Park, et al., Highly stretchable and conductive conductors based on ag flakes and polyester composites, Microelectron. Eng. 199 (2018) 16–23, https://doi.org/10.1016/j.mee.2018.07.006.
[28] IPC, IPC-9204 Guidelines on Flexibility and Stretchability Testing for Printed Electronics, 2017.
[29] ASTM International, ASTM F3147–15: Standard Test Method for Evaluating the Reliability of Surface Mounted Device (SMD) Joints on a Flexible Circuit by a Rolling Mandrel Bend, West Conshohocken, PA, USA, 2015.

[30] A. Korhonen, Master Thesis: Reliability Testing on Stretchable Electronics - Printed Conductors under Strain, University of Oulu, Oulu, Finland, 2019.

[31] T. Happonen, Doctoral Dissertation: Reliability Studies on Printed Conductors on Flexible Substrates under Cyclic Bending, University of Oulu, Oulu, Finland, 2016.

[32] J.A.V. Fraunhofer, Adhesion and cohesion, Int'l J. Density 951324 (2012), https://doi.org/10.1155/2012/951324.